

Giovanni NICOLETTI^{1,2}
 Marco Mario TRESOLDI^{1,3}
 Anna Maria GATTI⁴
 Margherita SANDANO⁵
 Manuela AGOZZINO⁶
 Laura VILLANI⁶
 Angela FAGA²
 Michelangelo BUONOCORE⁴

¹ Plastic and Reconstructive Surgery, Department of Clinical Surgical, Diagnostic and Pediatric Sciences, University of Pavia, Viale Brambilla, 74, 27100 Pavia, Italy

² Advanced Technologies for Regenerative Medicine and Inductive Surgery Research Center, University of Pavia, Viale Brambilla, 74, 27100 Pavia, Italy

³ Department of Surgery, Istituti Clinici Scientifici Maugeri SB SpA IRCCS, Via Salvatore Maugeri 10, 27100 Pavia, Italy

⁴ Clinical Neurophysiology Unit, Istituti Clinici Scientifici Maugeri SB SpA IRCCS, Via Salvatore Maugeri 10, 27100 Pavia, Italy

⁵ General Surgery Residency Program, University of Trieste, Azienda Sanitaria Universitaria Integrata di Trieste, Ospedale Cattinara, Strada di Fiume 447, Trieste 34149, Italy

⁶ Pathological Anatomy and Histology Unit, Istituti Clinici Scientifici Maugeri SB SpA IRCCS, Via Salvatore Maugeri 10, 27100 Pavia, Italy

Reprints: Giovanni Nicoletti
 <giovanni.nicoletti@unipv.it>

Article accepted on 02/09/2020

Pathological nerve patterns in human basal cell carcinoma

Background: The peculiar combined, or binary involvement of epithelium and stroma makes basal cell carcinoma (BCC) a unique tumour. Nerve fibres have been shown to play an active role in different cancers. **Objective:** A prospective observational study was carried out on punch biopsies harvested within BCC surgical excision specimens. **Materials & Methods:** A total of 10 samples of histologically diagnosed BCC, derived from 10 different patients (five females, five males), was included in the study. Within the BCCs, seven different histological sub-types were identified: morphea-like, basosquamous, micronodular, mixed nodular-micronodular, adenoid, nodular and superficial multifocal. Nerve fibres were stained for indirect immunofluorescence targeting protein gene product 9.5. **Results:** Three different morphological patterns of nerve fibre distribution within the BCCs were identified. Pattern 1 displayed a normal skin nerve pattern, in which the fibres were dislodged by the growing tumour masses. Pattern 2 featured a ball of curved, tangled nerve fibres close to the tumour masses, slightly resembling piloneural collar nerve fibres, wrapped around hair follicles in the normal anatomical setting. Pattern 3 showed nerve fibres crowding in the sub-epidermal layer with focal epidermal hyperinnervation. Such a pattern is reminiscent of the typical anatomical neuro-epithelial interaction in mechanosensory organs. **Conclusion:** Our study may disclose a hidden third player, of nerves. Thus, tissue involvement of BCCs may be better represented by the triad of epithelium, stroma and nerves, each component retaining some features associated with its developmental setting.

Key words: basal cell carcinoma, embryogenesis, nerve, skin cancer, skin adnexa, skin innervation

Several reports have demonstrated the active role of nerve fibres in the tumour microenvironment of different cancers [1-5] through a direct exchange between tumours and nerve fibres [6]. Tumours influence the extracellular environment through neurotrophic mediators, while, peri-tumoral nerve fibres release neuro-transmitters in proper neuro-neoplastic synapses, enhancing tumour development and progression [7-11]. Basal cell carcinoma (BCC) is the most common of all cancers. The aim of this study was to perform a detailed investigation of the anatomical interactions between nerve fibres and BCCs, both in the tumour mass and in the peri-tumoral environment.

Materials and methods

A prospective observational study was carried out in cooperation with the Plastic Surgery Unit of the University of Pavia (Italy), the Pathological Anatomy Section Laboratory and the Neurophysiology Laboratory of the ICS Maugeri

SB SpA IRCCS in Pavia (Italy). The study conformed to the 1975 Declaration of Helsinki; informed written consent was obtained from all of the patients and the trial was approved by the Ethics Committee of the Istituti Clinici Scientifici Maugeri SB SpA IRCCS, Pavia (Italy) (project identification code 2198).

The inclusion criteria were:

- Patients aged 18 or over.
- BCC sized 6 mm or more.
- Any anatomical site.

The exclusion criteria were:

- BCC sized less than 6 mm.
- Recurrent and/or persistent BCC on a scar.
- Unclear histological diagnosis.
- Patients with multiple neoplasms and/or genetic diseases.

Over a period of six months, from October 2017 to March 2018, a total of 10 samples of histologically diagnosed BCC, derived from 10 different patients (five females and

five males; age: mean 64.2, median 74), was included in the study.

Surgical excisions of clinically diagnosed BCCs were carried out with a 5-mm margin in healthy tissue according to the Italian Association of Medical Oncology (AIOM) 2017 guidelines. Two 3-mm punch biopsies, including the skin and the subcutaneous layers, were harvested for each surgical specimen. One 3-mm punch biopsy was harvested within the tumour mass, while the other was harvested in the clinically healthy skin around the tumour. The punch biopsies never extended to either the superficial or the deep margins of the surgical specimen, thus preventing any bias in the oncological diagnosis by the pathologist.

Haematoxylin and eosin staining

The surgical specimens were fixed with 10% neutral buffered formalin (pH 7.2) (Bio-Optica, Milan, Italy) for 24 hours at room temperature, and were then dehydrated through graded concentrations of ethanol (ASP300S Leica Microsystems Srl, Buccinasco, Milan, Italy) and embedded in paraffin. Subsequently, 3- μ m-thick sections were obtained with an automatic microtome (HM355S Thermo Fisher Scientific, Waltham, MA, USA), rehydrated and subsequently processed with Harry's Hematoxylin (Bio-Optica) for 4 minutes and Eosin (Bio-Optica) for 4 minutes at room temperature (ST5020 and CV5030 Leica Microsystems).

Immunofluorescence staining

The punch biopsies were fixed with Zamboni solution (2% paraformaldehyde and picric acid) at 4 °C for 24 hours and subsequently cryoprotected in a 20% sucrose solution with a 7.4 pH saline phosphate buffer. The samples were then placed in Optimum Cutting Temperature (OCT) gel and sliced in 50- μ m sections using a microtome provided with a refrigerating unit, working at -19 °C (HMG 450, Microm International, Walldorf, Germany).

Nerve fibres were stained for indirect immunofluorescence using primary rabbit polyclonal antibodies targeting protein gene product 9.5 (PGP 9.5). A secondary, species-specific antibody targeting the primary antibody was linked with cyanine 3 (Cy3), a fluorochrome of the cyanine family. Cyanine 3 displays green light with a maximum absorbance at 550 nm and a maximum light emission at 570 nm (yellow-orange). The dermal-epidermal junction was stained with a primary, mouse monoclonal antibody, targeting collagen IV fibres that are specific to the basal membrane. The species-specific secondary antibody targeting the primary antibody was linked to cyanine 2 (Cy2) fluorochrome which displays blue light, with maximum absorbance at 498 nm and maximum light emission at 505 nm (green) [12].

The sections were observed with a fluorescence microscope (Axioskop 40 FL, Zeiss, Gottingen, Germany) equipped with a digital camera (Axiocam MRC5, Zeiss) and dedicated image processing software (Axiovision Rel 4.8).

Results

In our sample, haematoxylin and eosin staining demonstrated seven different histological sub-types of BCC: four were classified as histologically aggressive according to Sexton [13] (one morphea-like, one basosquamous, one micronodular, two mixed nodular-micronodular) and three were histologically non-aggressive (two adenoid, two nodular, one superficial multifocal).

Overall, 247 stained micro-sections were analysed under the fluorescence microscope.

The immunofluorescence staining demonstrated the complete absence of nerve fibres within the tumour parenchyma in all of the samples. The nerve fibres were evident only within the stromal collagen.

Three different morphological patterns of nerve fibre distribution were identified at the interface between the tumour parenchyma and stromal collagen. A number of patterns coexisted in the same section in all of the samples (minimum of two, maximum of three).

Pattern 1 displayed normal nerve fibres that were dislodged by the tumour masses. Occasionally, stromal septa, including nerve fibres, were found to divide the tumour masses into multiple lobes (figure 1). Pattern 2 featured a chaotic aggregation of thin curved and tangled nerve fibres in the peritumoral stroma (Figures 2, 3). There was no correlation between Patterns 1 and 2 and any of the histological types. Pattern 3 was demonstrated only in the nodular BCCs, and featured a localized crowding of nerve fibres running between the tumour and the overlying epidermis. The fibres penetrated into the epidermis and focal epidermal hyperinnervation was appreciated. The nerve fibres also displayed some focal swelling that might be related to axon degeneration (figure 4).

Discussion

The onset of BCCs has been demonstrated to occur preferentially at sites of congenital craniofacial and neck clefts, which, in adulthood likely correspond to the sites of fusion and/or merging of embryonic processes [14-17]. Similarly, anomalies in the Hedgehog (Hh) signalling pathway play a major role in craniofacial congenital malformations [18, 19], from survival of migrating cranial neural crest cells [20] to fusion of craniofacial prominences [21-26].

Dysregulation of the Hh signalling pathway has been demonstrated in human BCC [27-30]. During both development and homeostasis, the Hh signalling pathway is finely tuned by a balance of upstream factors that can either promote its activation, such as Smoothened (SMO), or suppress it, such as Patched1 (PTCH1). In BCC, this balance is markedly tilted in favour of pathway activation through mutations yielding either loss of PTCH1 function, or, the stable activation of SMO [31, 32]. Evidence of a perturbed Hh signalling pathway in human BCC was indicated in studies demonstrating that patients with defective *PTCH1* alleles are predisposed to developing multiple BCCs (Gorlin's syndrome) [31, 33, 34].

Recently, Peterson *et al.* (2015) [35] demonstrated in *PTCH1*-deleted mice, treated with tamoxifen, that BCC was more likely to develop from specific cell clusters, defined

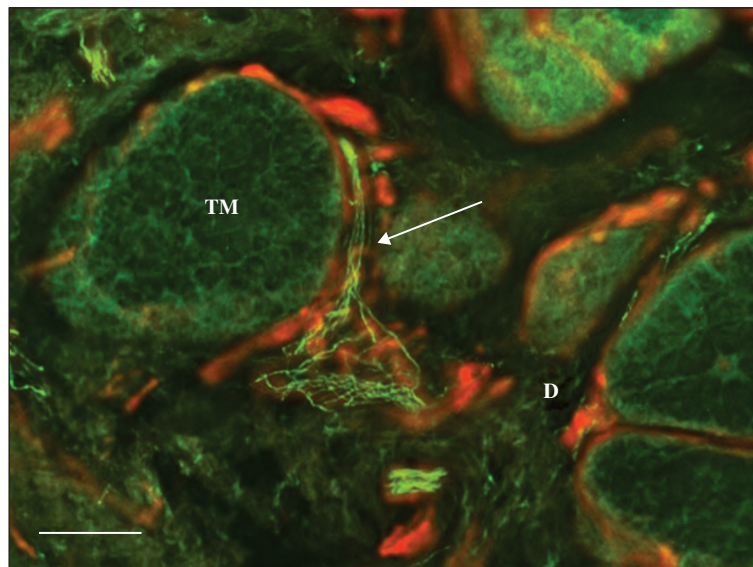


Figure 1. Pattern 1 showing a nerve fibre repositioning (arrow) due to the mechanical pressure of a tumour mass (TM). Green: PGP 9.5 staining of nerve fibres; red: type IV collagen staining of connective tissue (blood vessels). D: dermis. Bar: 100 µm.

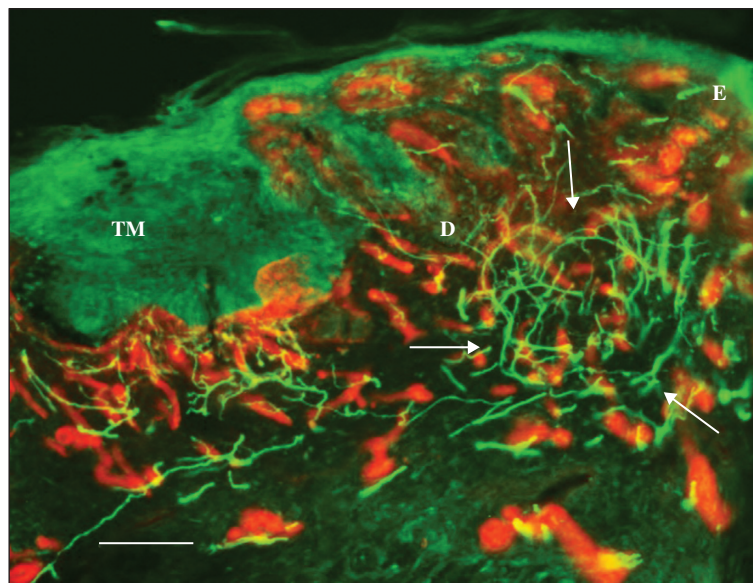


Figure 2. Pattern 2 showing a nerve fibre tangle (small arrows) in the dermis (D), not far from a tumour mass (TM). Green: PGP 9.5 staining of nerve fibres; red: type IV collagen staining of connective tissue (blood vessels). E: epidermis. D: dermis. Bar: 100 µm.

as “hot spots”. More specifically, neoplastic degeneration was demonstrated in upper and lower bulge stem cells of the hair follicle, and in small inter-follicular cell clusters close to highly innervated zones called “touch domes” (TDs). Within the hair follicle, the nerve fibres form the so-called “piloneural collar”. A sort of delicate basket, it includes a variety of sensory afferents and terminal Schwann cells that innervate a region below the sebaceous gland, but above the hair follicle upper bulge [36]. The piloneural collar is typically structured in an inner layer of nerve fibres which run in a longitudinal direction forming palisades of lanceolate nerve endings, and an outer layer of fibres with a circumferential pattern.

The TDs are specialized structures in the papillary dermis of hair-bearing skin that approach the hair follicle without penetrating it. They are made of specialized Merkel cells that detect and transmit light and touch sensations through the underlying slowly adapting type 1 sensory afferent nerve fibres [37, 38]. In the TDs, the nerve fibres approach the epidermis, branching into smaller fibres that crowd in the sub-epidermal region, eventually penetrating the epidermis to join Merkel cells [39-41].

According to Peterson (2015) [35], direct involvement of the nervous system in the development of BCC, as well as in other malignancies [4], might be suggested, as the skin “hot spots” display a tight interconnection

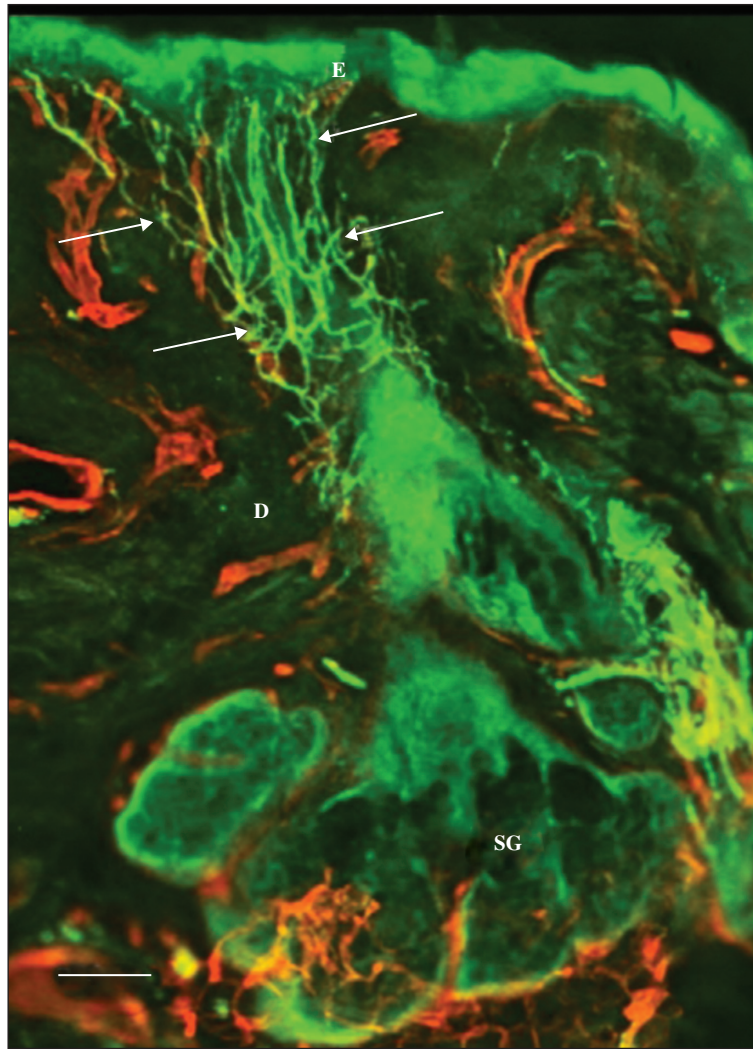


Figure 3. A nerve fibre bundle (small arrows) in the dermis (D), from the apex of a sebaceous gland (SG) to the epidermis (E). Green: PGP 9.5 staining of nerve fibres; red: type IV collagen staining of connective tissue (mainly blood vessels). Bar: 100 μ m.

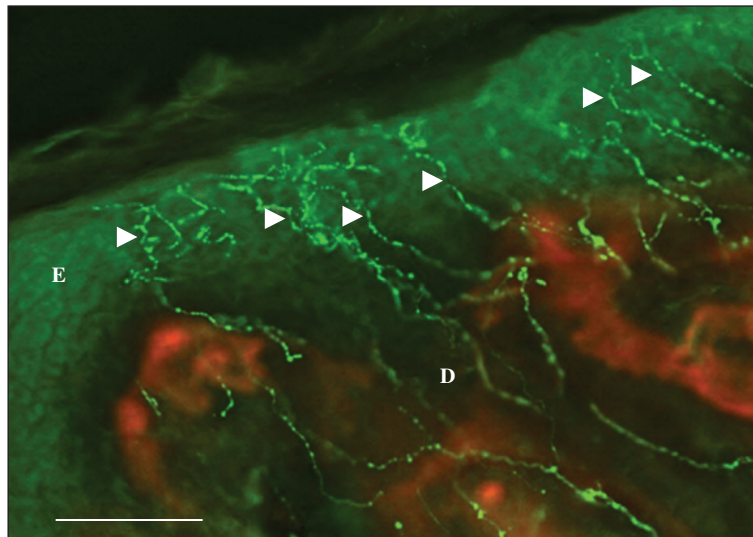


Figure 4. Pattern 3 showing clear hyperinnervation of the epidermis with an increased density of epidermal nerve fibres (arrow-heads). Green: PGP 9.5 staining of nerve fibres; red: type IV collagen staining of connective tissue (blood vessels). E: epidermis. D: dermis. Bar: 100 μ m.

with the nervous tissue. Their study demonstrated that the skin-sensitive nerve fibres express the Hedgehog ligand, and that the skin denervation interferes with Hh activity in the TDs, blunting tumour development and progression from these cells. These results suggest that the skin nerve endings produce the Hh ligand that, in turn, triggers tumour development at the TD site. Nevertheless, as TD-derived tumours do not respond to anti-Hh ligand antibodies, the involvement of multiple different types of Hh ligands might be hypothesized in the process of cancer development. Thus, in order to prevent the Hh-ligand carcinogenic effect, it would seem appropriate to deactivate the Hh receptor with permanent denervation [35]. Other studies, meanwhile, have demonstrated that the Hh pathway might also be activated by TGF-beta [42].

Our observations demonstrate a total of three morphological nerve patterns within BCC samples. Pattern 1 did not show actual pathological features, as it displayed a normal skin nerve pattern in which the fibres were simply dislodged and splayed by the growing tumour masses. Patterns 2 and 3, on the other hand, displayed a clear pathological trait: Pattern 2 featured a ball of curved, tangled nerve fibres close to the tumour masses resembling the piloneural collar nerve fibres that wrap around the hair follicle in the normal anatomical setting. Pattern 3, meanwhile, showed nerve fibre crowding in the sub-epidermal layer with the fibres approaching the epidermis. Such a pattern might call to mind the typical anatomical neuro-epithelial interaction in a TD.

Our study failed to demonstrate a correlation between the different nerve distribution patterns and the histological types of BCCs and their clinical variations. Undoubtedly, a larger sample could potentially demonstrate more reliable results. However, the comparative complexity of the coordinated clinical and experimental setting, we believe, justifies the small-sized sample in our trial.

The epidermis and skin adnexa share the same ectodermal origin as nerve tissue, and in adult skin they demonstrate a close mutual anatomical and functional interaction.

The peculiar combined, or binary, involvement of epithelium and stroma makes BCC a unique tumour versus other epithelial malignancies, in which individual epithelial cells transform into cancer cells that subsequently feature a stroma-dissociated invasiveness [43]. On the other hand, skin adnexal primordial tissue with combined fibro-epithelial growth is always retained in BCC. Such a unique pattern supports the alternative concept of a monstrous attempt at skin adnexogenesis in BCC in adults, rather than proper malignancy [44]. Therefore, considering the common neuro-ectodermal origin of both the epidermis and nerves, a mutual active interaction between these tissues might be expected in BCC.

Our study may have disclosed a hidden third player, of nerves, thus, rather than binary tissue interaction in BCC, the following triad may be involved: the epithelium, stroma and nerves, with each component potentially retaining some features associated with its developmental setting. The protective effect resulting from selective denervation, based on BCC in experimental animals, might be explained by suppression of one of the tissues actively involved in mutually interactive development and proliferation. Therefore, in the specific case of BCC, nerves might be one element in the context of combined organoid proliferation, rather than direct carcinogenetic inducers [35].

Such evidence may provide further support to the hypothesis of embryological pathogenesis of BCC, and perhaps lead to suggestions for novel preventive and therapeutic proposals.

Acknowledgements and disclosures. *Acknowledgements: The Authors wish to thank Morag McGhee (MA) and Eleanor Susan Lim (MA, Hons) for their contribution to the submission of this dissertation. Financial support: none. Conflicts of interest: none.*

References

1. Nodl F. Das periphere Nervengewebe in der Histogenese des Basalioms. *Arch Klin Exp Dermatol* 1962; 214: 337-45.
2. Ormea F, Bossi G, Garcovich A. Contributo allo studio dell'ultrastruttura delle neoplasie epiteliali cutanee [Contribution to the study of the ultrastructure of cutaneous epithelial neoplasms]. *Minerva Dermatol* 1968; 43: 683-724.
3. Pawlowski A. Rola elementów nerwowych skóry w przebiegu doświadczalnej karcinogenezy, oraz nabłoniaków podstawnokomórkowych i raków kolczystokomórkowych u ludzi [The role of nerve elements of the skin in the course of experimental carcinogenesis and of basal cell epithelioma and squamous cell carcinoma in man]. *Neuropatol Pol* 1970; 8: 205-39.
4. Panuncio A, Vignale R, Lopez G. Immunohistochemical study of nerve fibres in basal cell carcinoma. *Eur J Dermatol* 2003; 13: 250-3.
5. Campbell LK, Thomas JR, Lamps LW, Smoller BR, Folpe AL. Protein gene product 9.5 (PGP 9.5) is not a specific marker of neural and nerve sheath tumors: an immunohistochemical study of 95 mesenchymal neoplasms. *Mod Pathol* 2003; 16: 963-9.
6. Jobling P, Pundavela J, Oliveira SMR, Roselli S, Walker MM, Hondermarck H. Nerve-cancer cell cross-talk: a novel promoter of tumor progression. *Cancer Res* 2015; 75: 1777-81.
7. Magnon C, Hall SJ, Lin J, et al. Autonomic nerve development contributes to prostate cancer progression. *Science* 2013; 341: 1236361.
8. Zhao C-M, Hayakawa Y, Kodama Y, et al. Denervation suppresses gastric tumorigenesis. *Sci Transl Med* 2014; 6: 250ra115.
9. Saloman JL, Albers KM, Li D, et al. Ablation of sensory neurons in a genetic model of pancreatic ductal adenocarcinoma slows initiation and progression of cancer. *Proc Natl Acad Sci USA* 2016; 113: 3078-83.
10. Horvathova L, Padova A, Tillinger A, Osacka J, Bizik J, Mravec B. Sympathectomy reduces tumor weight and affects expression of tumor-related genes in melanoma tissue in the mouse. *Stress* 2016; 19: 528-34.
11. Lackovicova L, Banovska L, Bundzikova J, et al. Chemical sympathectomy suppresses fibrosarcoma development and improves survival of tumor-bearing rats. *Neoplasma* 2011; 58: 424-9.
12. Lauria G, Cornblath DR, Johansson O, et al. EFNS guidelines on the use of skin biopsy in the diagnosis of peripheral neuropathy. *Eur J Neurol* 2005; 12: 747-58.
13. Sexton M, Jones DB, Maloney ME. Histologic pattern analysis of basal cell carcinoma. Study of a series of 1039 consecutive neoplasms. *J Am Acad Dermatol* 1990; 23: 1118-26.
14. Newman JC, Leffell DJ. Correlation of embryonic fusion planes with the anatomical distribution of basal cell carcinoma. *Dermatol Surg* 2007; 33: 957-65.
15. Nicoletti G, Brenta F, Malovini A, Jaber O, Faga A. Sites of basal cell carcinomas and head and neck congenital clefts: topographic correlation. *Plast Reconstr Surg Glob Open* 2014; 2: e164.

16. Nicoletti G, Tresoldi MM, Malovini A, Prigent S, Agozzino M, Faga A. Correlation between the sites of onset of basal cell carcinoma and the embryonic fusion planes in the auricle. *Clin Med Insights Oncol* 2018; 12: 1179554918817328.
17. Nicoletti G, Tresoldi MM, Malovini A, Borelli F, Faga A. Nonmelanoma skin cancers: embryologically relevant sites and UV exposure. *Plast Reconstr Surg Glob Open* 2020; 8: e2683.
18. Metzis V, Courtney AD, Kerr MC, et al. Patched 1 is required in neural crest cells for the prevention of orofacial clefts. *Hum Mol Genet* 2013; 22: 5026-35.
19. Abramyan J. Hedgehog signaling and embryonic craniofacial disorders. *J Dev Biol* 2019; 7: 9.
20. Ahlgren SC, Bronner-Fraser M. Inhibition of sonic hedgehog signaling in vivo results in craniofacial neural crest cell death. *Curr Biol* 1999; 9: 1304-14.
21. Cobourne MT, Green JB. Hedgehog signalling in development of the secondary palate. *Front Oral Biol* 2012; 16: 52-9.
22. Xavier GM, Seppala M, Barrell W, Birjandi AA, Geoghegan F, Cobourne MT. Hedgehog receptor function during craniofacial development. *Dev Biol* 2016; 415: 198-215.
23. Dworkin S, Boglev Y, Owens H, Goldie SJ. The role of sonic hedgehog in craniofacial patterning, morphogenesis and cranial neural crest survival. *J Dev Biol* 2016; 4: 24.
24. Kurosaka H. The roles of hedgehog signaling in upper lip formation. *Biomed Res Int* 2015; 2015: 901041.
25. Seppala M, Fraser GJ, Birjandi AA, Xavier GM, Cobourne MT. Sonic hedgehog signaling and development of the dentition. *J Dev Biol* 2017; 5: 6.
26. Lan Y, Jiang R. Sonic hedgehog signaling regulates reciprocal epithelial-mesenchymal interactions controlling palatal outgrowth. *Development* 2009; 136: 1387-96.
27. Epstein EH. Basal cell carcinomas: attack of the hedgehog. *Nat Rev Cancer* 2008; 8: 743-54.
28. Epstein EH Jr.. Mommy - where do tumors come from? *J Clin Invest* 2011; 121: 1681-3.
29. Kasper M, Jaks V, Are A, et al. Wounding enhances epidermal tumorigenesis by recruiting hair follicle keratinocytes. *Proc Natl Acad Sci USA* 2011; 108: 4099-104.
30. Kasper M, Jaks V, Hohl D, Toftgård R. Basal cell carcinoma - molecular biology and potential new therapies. *J Clin Invest* 2012; 122: 455-63.
31. Johnson RL, Rothman AL, Xie J, et al. Human homolog of patched, a candidate gene for the basal cell nevus syndrome. *Science* 1996; 272: 1668-71.
32. Xie J, Murone M, Luoh SM, et al. Activating smoothened mutations in sporadic basal-cell carcinoma. *Nature* 1998; 391: 90-2.
33. Bonifas JM, Bare JW, Kerschmann RL, Master SP, Epstein EH Jr.. Parental origin of chromosome 9q22.3-q31 lost in basal cell carcinomas from basal cell nevus syndrome patients. *Hum Mol Genet* 1994; 3: 447-8.
34. Hahn H, Wicking C, Zaphiropoulos PG, et al. Mutations of the human homolog of Drosophila patched in the nevoid basal cell carcinoma syndrome. *Cell* 1996; 85: 841-51.
35. Peterson SC, Eberl M, Vagnozzi AN, et al. Basal cell carcinoma preferentially arises from stem cells within hair follicle and mechanosensory niches. *Cell Stem Cell* 2015; 16: 400-12.
36. Woo SH, Baba Y, Franco AM, Lumpkin EA, Owens DM. Excitatory glutamate is essential for development and maintenance of the piloneural mechanoreceptor. *Development* 2012; 139: 740-8.
37. Maricich SM, Wellnitz SA, Nelson AM, et al. Merkel cells are essential for light-touch responses. *Science* 2009; 324: 1580-2.
38. Maksimovic S, Nakatani M, Baba Y, et al. Epidermal Merkel cells are mechanosensory cells that tune mammalian touch receptors. *Nature* 2014; 509: 617-21.
39. Arthur RP, Shelley WB. The innervation of human epidermis. *J Invest Dermatol* 1959; 32: 397-411.
40. Kennedy WR, Wendelschafer-Crabb G. The innervation of human epidermis. *J Neurol Sci* 1993; 115: 184-90.
41. Halata Z, Grim M, Bauman KI. Friedrich Sigmund Merkel and his "Merkel cell", morphology, development, and physiology: review and new results. *Anat Rec A Discov Mol Cell Evol Biol* 2003; 271: 225-39.
42. Nolan-Stevaux O, Lau J, Truitt ML, et al. GLI1 is regulated through smoothened-independent mechanisms in neoplastic pancreatic ducts and mediates PDAC cell survival and transformation. *Genes Dev* 2009; 23: 24-36.
43. Pinkus H. Adnexal tumors, benign, not-so-benign and malignant. *Adv Biol Skin* 1966; 7: 255-76.
44. Callahan CA, Oro AE. Monstrous attempts at adnexogenesis: regulating hair follicle progenitors through Sonic hedgehog signaling. *Curr Opin Genet Dev* 2001; 11: 541-6.